Published in final edited form as:
Science. 2014 January 24; 343(6169): 419–422. doi:10.1126/science.1242939.

Single β-Actin mRNA Detection in Neurons Reveals a Mechanism for Regulating Its Translatability

Adina R. Buxbaum[1,2], **Bin Wu**[1,2], and **Robert H. Singer**[1,2,3,4,*]

[1]Department of Anatomy and Structural Biology, Albert Einstein College of Medicine, 1300 Morris Park Avenue, Bronx, NY 10461, USA

[2]Gruss Lipper Biophotonics Center, Albert Einstein College of Medicine, 1300 Morris Park Avenue, Bronx, NY 10461, USA

[3]Dominick P. Purpura Department of Neuroscience, Albert Einstein College of Medicine, 1300 Morris Park Avenue, Bronx, NY 10461, USA

[4]Janelia Farm Research Campus, Howard Hughes Medical Institute, Ashburn, VA 20147, USA

The physical manifestation of learning and memory formation in the brain can be expressed by strengthening or weakening of synaptic connections through morphological changes. Local actin remodeling underlies some forms of plasticity and may be facilitated by local b-actin synthesis, but dynamic information is lacking. In this work, we use single-molecule in situ hybridization to demonstrate that dendritic b-actin messenger RNA (mRNA) and ribosomes are in a masked, neuron-specific form. Chemically induced long-term potentiation prompts transient mRNA unmasking, which depends on factors active during synaptic activity. Ribosomes and single b-actin mRNA motility increase after stimulation, indicative of release from complexes. Hence, the single-molecule assays we developed allow for the quantification of activity-induced unmasking and availability for active translation. Further, our work demonstrates that b-actin mRNA and ribosomes are in a masked state that is alleviated by stimulation.

More than a century ago, Ramón y Cajal postulated that memories could be stored by modifying the shape and, consequently, the strength of synaptic connections between neurons (1). In our current understanding of learning and memory formation, synaptic plasticity expressed as activity-induced changes in synapse morphology and, subsequently, in signaling strength constitutes one of the physical manifestations of memory formation (2). In postsynaptic forms of plasticity, activity-induced morphological remodeling and

*Corresponding author: robert.singer@einstein.yu.edu.

Supplementary Materials
Materials and Methods
Figs. S1 to S9
References
FISH Probe Sequences
Movies S1 and S2

A.R.B., B.W., and R.H.S. designed the experiments; A.R.B. performed the experiments; A.R.B. and B.W. performed optical engineering and data analysis; and A.R.B. and R.H.S. wrote the manuscript. Data in this paper are in partial fulfillment of the Ph.D. degree to A.R.B.

enhanced synaptic transmission can be specific to a single dendritic spine (3) and can require both protein synthesis (4) and increased polymerization of the cytoskeletal protein β-actin (5). Local protein synthesis provides a mechanism of achieving spatial specificity of synaptic modification that can persist over time (6). β-actin mRNA localization in neuronal dendrites is essential for proper dendritic spine structure and abundance (7, 8), suggesting that regulation of β-actin protein concentration through local translation plays a role in synaptic plasticity.

Because β-actin mRNA is abundant in neurons (9), mRNAs must be maintained in a repressed state in the vicinity of synapses with translation factors readily available as needed for local translation. Physical sequestration of localized mRNAs in large neuronal RNA granule structures may serve to repress the mRNAs. RNA granules have been described as large, dense, neuronal-specific structures composed of ribosomes; mRNAs, including β-actin mRNA; and translation factors (10, 11). Putatively, local activity induces granule disassembly, spatially restricting translation to stimulated synapses (10, 12). To date, there exists little evidence that granules regulate mRNA functionality. With the use of single-molecule imaging of endogenous β-actin mRNA and ribosomes, we provide evidence that the availability of β-actin mRNA to translation factors is transiently regulated by synaptic activity.

Single mRNA fluorescent in situ hybridization (FISH) analysis provided an absolute quantitation of dendritic mRNAs in cultured hippocampal neurons (13) (fig. S1). Probe hybridization efficiency to single molecules was calibrated with the brightness of a single probe (14). By this method, we found that dendritic mRNAs bind only half of the expected probes (Fig. 1, A and D, and fig. S2). However, exposure to chemical long-term potentiation (cLTP) induction, known to result in enlarged spines (15), increased probe binding to the expected number (11) and doubled detection of β-actin mRNAs along dendrites within 10 to 15 min (Fig. 1, B, D, and E; fig. S2, A and C; and fig. S3). Inefficient mRNA detection suggested inaccessibility of probes to dendritic mRNA, whereas stimulation induces unmasking. In contrast to neurons, β-actin mRNAs in glial cells in the same field hybridized the expected number of probes, irrespective of stimulation (fig. S2B). Probes to the β-actin 3′ untranslated region (3′UTR), as well as the open reading frame, demonstrated mRNA unmasking (fig. S2, C and D). Increased mRNA was not due to transport from the soma or transcription (fig. S2, E to G).

If mRNA was masked by a proteinaceous complex, a limited prehybridization proteolytic digestion step would be expected to enhance mRNA detection. A protease digestion protocol was devised (16) that increased detectable β-actin mRNAs in dendrites equivalent to levels after stimulation (Fig. 1E). Poly(A) mRNA detection in dendrites also increased upon digestion (fig. S2H), suggesting that additional mRNAs may be masked in neurons.

To be physiologically regulated, mRNA unmasking would require signaling cascades that occur during synaptic activity. Inhibition of N-methyl-d-aspartate (NMDA) receptor activity with 2-amino-5-phosphonopentanoic acid (APV), inhibition of MEK1/2 (mitogen-activated protein kinase kinase 1 and 2) with UO-126, or depletion of calcium from the extracellular medium prevented increased mRNA detection during cLTP (Fig. 1, F and G), relating

NIH-PA Author Manuscript

NIH-PA Author Manuscript

mRNA unmasking to local metabolic changes that occur during synaptic plasticity. Detectable dendritic β-actin mRNA peaked at 10 min after cLTP and returned to baseline within 30 min (Fig. 1G), indicating that the default condition is masking. Furthermore, limited mRNA availability for translation after cLTP could provide for a burst of protein synthesis.

Because repressive RNA granule complexes in neurons are composed of densely packed ribosomes (11), ribosomes may also be unmasked during cLTP. Similar to mRNA, cLTP increased endogenous ribosomal RNA (rRNA) detection along dendrites, as did sample digestion (Fig. 2A and fig. S4, A to E). Ribosomal particle intensities in protease-treated neuronal dendrites were nonhomogeneous and contained denser regions when compared with glia (fig. S4, F to H). Consistent with dispersal of ribosomes during unmasking, cLTP decreased the abundance of bright dendritic rRNA structures (fig. S4, E and I, and fig. S5F). To determine whether β-actin mRNA and ribosomes may be associated in the same particle as previously reported (11, 17), we performed dual-color hybridization in protease digested neurons (Fig. 2B). More than 30% of β-actin mRNAs colocalized with neuron-specific bright ribosomal structures.

Three-color imaging differentiated ribosome association with masked and unmasked mRNAs (fig. S5A). β-actin mRNAs hybridized with a second-color probe after protease digestion revealed previously masked mRNAs (about half of the total). Masked mRNAs were associated with brighter ribosomal puncta, supporting the hypothesis that regions rich in ribosomes are part of the same masked complex (Fig. 2C and fig. S5, B to D).

Unbound and unmasked molecules should be washed away during permeablization of live neurons. Puromycin eliminated actively translating polysomes, followed by detergent extraction and fixation (fig. S6A). Large, bright ribosomal puncta were retained in dendrites, some containing single β-actin mRNAs; in contrast, glial cytoplasmic ribosomal signal was extracted (fig. S6, B to D and H). After cLTP in detergent-treated neurons, ribosome and β-actin mRNA FISH signal (Fig. 2D and fig. S6E) and the size of the optically reconstructed ribosomal puncta (fig. S6, F and G) decreased by about half, consistent with increased dispersal of ribosomes and mRNAs as a result of synaptic stimulation.

Increased ribosomal dispersal due to unmasking resulted in increased diffusion of ribosomes and mRNAs. To investigate dendritic rRNA dynamics, we employed spot photoactivation of a ribosomal protein (L10A) fusion. Immobile, bright structures surrounded single mRNAs (Fig. 2E). Photoactivated ribosome fusions exhibited diminished motility in dendrites relative to glial cells (Fig. 2G). After cLTP, quantification of ribosome dispersal from photoactivated sites revealed that the immobile ribosome fraction decreased (fig. S7B). Dendritic β-actin mRNAs were immobile, with a small portion undergoing active transport (18). Upon stimulation, immobile mRNAs exhibited corralled diffusion in their local environment (fig. S7, C and D), consistent with degranulation of a complex that prevents mRNA from diffusing until synaptic stimulation.

In addition to increased mRNA and ribosome dynamics, cLTP increased protein synthesis of a reporter for β-actin mRNA, consistent with unmasking that correlates with increased local β-actin translation (fig. S8). The protein FMRP has been shown to be a component of RNA granules and stalls ribosomes on mRNAs (19). Fmr1 knockout brains exhibit a reduction in the postpolysomal fractions (20), suggesting a role for Fmr1 in granule integrity. Accordingly, Fmr1 knockdown in culture decreased the abundance of masked β-actin mRNAs (fig. S9, A to C). We observed a similar effect in neurons isolated from knockout animals lacking the β-actin mRNA binding protein ZBP1 (fig. S9D).

In the model supported by this work, β-actin mRNA is present all along dendrites and is kept in a dormant state by packaging into inert structures ready to be locally activated. During synaptic stimulation, downstream effectors of signaling pathways locally prompt complex disassembly, putatively allowing active translation of mRNAs at activated synapses. This could be accomplished by regulation of self-aggregating protein motifs through posttranslational modifications (21) facilitating cycles of localized RNA granule formation and degranulation, thus making use of the same mRNAs repeatedly over time.

Supplementary Material

Refer to Web version on PubMed Central for supplementary material.

Acknowledgments

We thank G. J. Bassell for the gift of the Dendra-actin 3′UTR construct, J. Du Hoffmann for invaluable programming help, D. R. Larson for Localize software, and Y. J. Yoon for cloning L10A and helpful discussions. We also thank T. Tr ek and other past and present members of the Singer lab for their suggestions and support. This work was supported by NIH grant NS083085-19 (formerly GM84364) and the Weisman Family Foundation.

References and Notes

1. Ramón y Cajal S. Proc R Soc London. 1894; 55:444–468.
2. Holtmaat A, Svoboda K. Nat Rev Neurosci. 2009; 10:647–658. [PubMed: 19693029]
3. Matsuzaki M, Honkura N, Ellis-Davies GC, Kasai H. Nature. 2004; 429:761–766. [PubMed: 15190253]
4. Tanaka J, et al. Science. 2008; 319:1683–1687. [PubMed: 18309046]
5. Ramachandran B, Frey JU. J Neurosci. 2009; 29:12167–12173. [PubMed: 19793974]
6. Sutton MA, Schuman EM. Cell. 2006; 127:49–58. [PubMed: 17018276]
7. Eom T, Antar LN, Singer RH, Bassell GJ. J Neurosci. 2003; 23:10433–10444. [PubMed: 14614102]
8. Klein ME, Younts TJ, Castillo PE, Jordan BA. Proc Natl Acad Sci USA. 2013; 110:3125–3130. [PubMed: 23382180]
9. Cajigas IJ, et al. Neuron. 2012; 74:453–466. [PubMed: 22578497]
10. Krichevsky AM, Kosik KS. Neuron. 2001; 32:683–696. [PubMed: 11719208]
11. Elvira G, et al. Mol Cell Proteomics. 2006; 5:635–651. [PubMed: 16352523]
12. Graber TE, et al. Proc Natl Acad Sci USA. 2013; 110:16205–16210. [PubMed: 24043809]
13. Materials and methods are available as supplementary materials on Science Online.
14. Zenklusen D, Larson DR, Singer RH. Nat Struct Mol Biol. 2008; 15:1263–1271. [PubMed: 19011635]
15. Lu W, et al. Neuron. 2001; 29:243–254. [PubMed: 11182095]
16. Kanai Y, Dohmae N, Hirokawa N. Neuron. 2004; 43:513–525. [PubMed: 15312650]
17. Knowles RB, et al. J Neurosci. 1996; 16:7812–7820. [PubMed: 8987809]
18. Park HY, et al. Science. 2014; 343:422–424. [PubMed: 24458643]
19. Darnell JC, et al. Cell. 2011; 146:247–261. [PubMed: 21784246]

20. Aschrafi A, Cunningham BA, Edelman GM, Vanderklish PW. Proc Natl Acad Sci USA. 2005; 102:2180–2185. [PubMed: 15684045]
21. Han TW, et al. Cell. 2012; 149:768–779. [PubMed: 22579282]

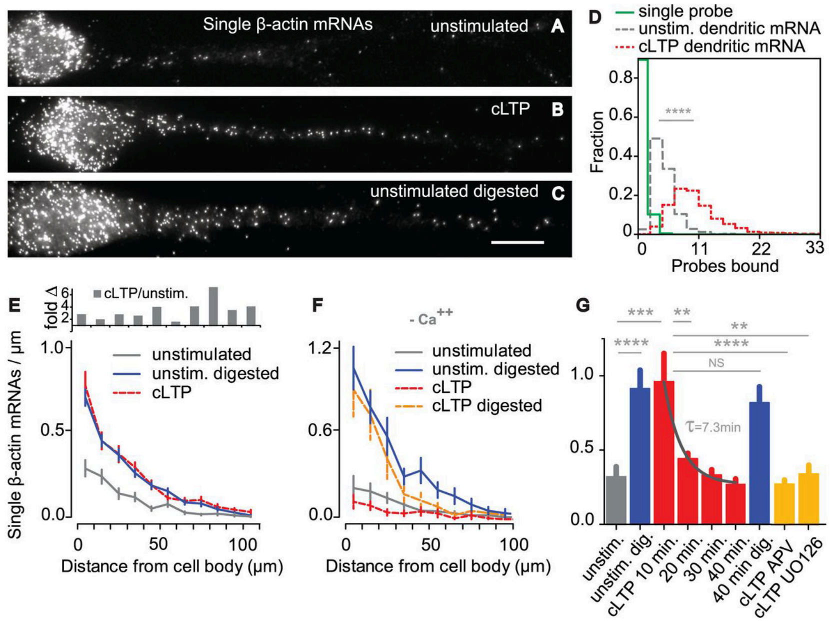

Fig. 1. Synaptic stimulation leads to increased detection of endogenous single β-actin mRNAs in dendrites

Single-molecule FISH of endogenous β-actin mRNAs in (**A**) unstimulated, (**B**) cLTP-stimulated, and (**C**) protease-digested cultured hippocampal neurons. Scale bar, 10 µm. (**D**) Histogram of integrated intensities of single β-actin mRNAs in dendrites. After cLTP, single mRNAs bind the expected number of probes, although half without stimulation (unstim.) [****P < 0.0001 (cLTP n = 2728 mRNAs, 25 cells; unstim. n = 665 mRNAs, 19 cells; single FISH probes n = 2131)]. (**E**) Single β-actin mRNAs per micrometer in dendrites. Fold increase of mRNA density along unstimulated to stimulated dendrites (top). From top to bottom in key: n = 26, 97, or 57 dendrites. (**F**) Single β-actin mRNAs per micrometer in dendrites with removal of extracellular calcium (from top to bottom: n = 23, 12, 19, or 7 dendrites). (**G**) Mean single mRNAs per micrometer in the first 50 µm of dendrites. cLTP-induced unmasking of mRNA decays with a time constant (τ) of 7.3 min (fit: coefficient of determination R^2 = 0.996). Digestion 40 min after cLTP shows no decrease in mRNA, consistent with mRNA repackaging (P = 0.5). Increased mRNA detection is blocked by NMDA receptor inhibition (APV) or MEK1/2 inhibition (UO126) (**P < 0.01, ***P = 0.001, ****P < 0.0001; Student's t test). In order from left to right: n = 26, 21, 21, 35, 47, 44, 32, 31, or 23 dendrites. NS, not significant; dig., digested. Error bars in (E) to (G) denote SEM.

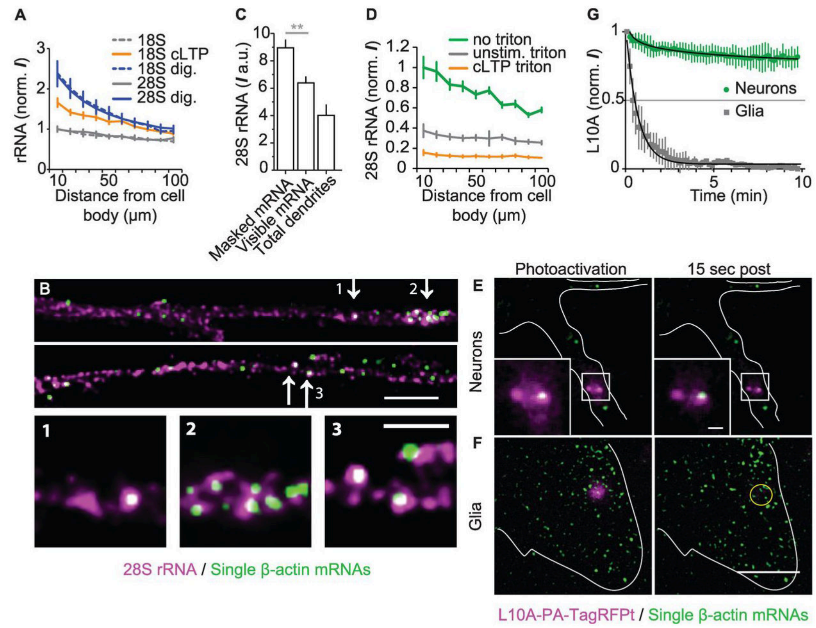

Fig. 2. Ribosomal complexes obscure β-actin mRNA

(**A**) Mean endogenous rRNA FISH fluorescence along dendrites (from top to bottom in key: *n* = 49, 30, 52, 92, or 97 dendrites). Signal normalized (norm.) to the first point of unstimulated data. Error bars denote SEM. I, intensity; dig., digested. (**B**) Single β-actin mRNAs and bright rRNA puncta often coincide (indicated by arrows). Scale bars, 5 μm (upper); 2 μm (lower). Numbers indicate magnified regions in bottom row. Magnified images were resampled with cubic convolution interpolation. (**C**) Mean dendritic ribosome signal surrounding mRNAs and total ribosomal signal (*n* = 38 dendrites, **P < 0.01; Student's t test). a.u., arbitrary units. (**D**) Mean dendritic rRNA FISH fluorescence in prefixative triton digested samples. Error bars indicate SEM. (**E**) Spot photoactivation of L10A-PA-TagRFPt at the site of β-actin mRNA in neurons revealed ribosome structures. Scale bar (inset), 1 μm. (**F**) In glia, L10A diffused away from the activated spot. Scale bar, 10 μm. (**G**) Loss of fluorescent L10A from photoactivated spot (*n* = 6 glia, 12 neurons). Error bars denote SD.